

INVESTIGATION OF A PENNING DISCHARGE
AT LOW PRESSURE

B.G. Safronov and V.G. Kononov

(NASA-TT-P-15523) INVESTIGATION OF A
PENNING DISCHARGE AT LOW PRESSURE (Kanner
(Leo) Associates) 16 p HC \$4.00

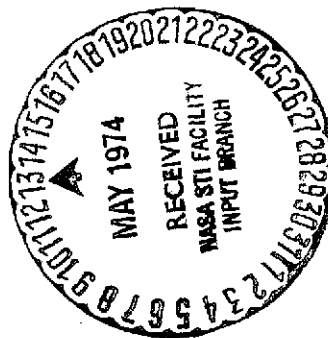
N74-22353

CSSL 201

G3/25

Unclass
37001

Translation of "Issledovaniye Penningovskogo razryada pri
nizkom davlenii," Fizika plazmy i problemy upravliyaemgo
termoyadernogo sinteza (Akademiya Nauk UkSSR, Kiev), No. 4,
1973, pp. 27-37



STANDARD TITLE PAGE

1. Report No. NASA TT F-15,523	2. Government Accession No.	3. Recipient's Catalog No.	
4. Title and Subtitle INVESTIGATION OF A PENNING DISCHARGE AT LOW PRESSURE		5. Report Date April 1974	
		6. Performing Organization Code	
7. Author(s) B.G. Safronov and V.G. Konovalov		8. Performing Organization Report No.	
		10. Work Unit No.	
9. Performing Organization Name and Address Leo Kanner Associates, P.O. Box 5187, Redwood City, California 94063		11. Contract or Grant No. NASW-2481	
		13. Type of Report and Period Covered Translation	
12. Sponsoring Agency Name and Address NATIONAL AERONAUTICS AND SPACE ADMINIS- TRATION, WASHINGTON, D.C. 20546		14. Sponsoring Agency Code	
15. Supplementary Notes Translation of "Issledovaniye Penningovskogo razryada pri nizkom davlenii," Fizika plazmy i problemy upravliyaemgo termoyadernogo sinteza (Akademiya Nauk UkSSR, Kiev), No. 4, 1973, pp. 27-37.			
16. Abstract The diamagnetism of a Penning-discharge plasma was studied experimentally as a function of gas pressure, magnetic field strength, and applied voltage. Results show that the diamagnetism of the plasma and the uncompensated current circulating near the anode are strongly dependent on the applied voltage. The ratio of the circulating current to the discharge current decreases with increasing gas pressure. The estimated 300-microsec energetic lifetime of the plasma at 0.1 microtorr pressure is in good correlation with the ionizational collision rate. Cathode sputtering patterns are examined to evaluate the transverse component of ion energy.			
17. Key Words (Selected by Author(s))		18. Distribution Statement Unclassified - Unlimited	
19. Security Classif. (of this report) Unclassified	20. Security Classif. (of this page) Unclassified	21. No. of Pages 16	22. Price 4.00

INVESTIGATION OF A PENNING DISCHARGE AT LOW PRESSURE

B.G. Safronov and V.G. Konovalov

Introduction

/27*

Despite the fact that the mechanism of a Penning discharge remains completely unexplained up to the present time, intensive experimental research on this type of discharge has led to diverse uses of it. It is an ion source, vacuum pump, manometer and, finally, particle counter [1].

The existence of two magnetic field discharge modes (at low and high magnetic field values) and two pressure discharge modes (a high voltage discharge at low pressure $<10^{-4}$ torr and a low voltage discharge at high pressure $>10^{-3}$ torr) should be considered definitely established at the present time [2]. It also has been noted that the transition from the high pressure mode to the low pressure mode takes place by jumps, as a result of which the noise in the discharge plasma decreases sharply.

Among the great number of published works, the work of Knauer [3] is of interest; in it, the formation of a rotating electron cloud of considerable density under high vacuum conditions was observed, as well as the escape of high energy ions across the magnetic field.

This work was undertaken to explain the possibility of creation of a plasma with high energy content.

Description of Unit and Methods of Investigation

The experimental unit is a regular Penning cell with the following dimensions: inner diameter of anode cylinder 2 cm,

*Numbers in the margin indicate pagination in the foreign text.

length 2.3 cm; cathode disk diameter 2.3 cm. The anode was /28
 fabricated from copper and the cathode plates of molybdenum. The
 entire system was assembled in holders on a metal flange. The
 electrical outlets were made with porcelain insulators. The
 vacuum chamber was made of stainless steel with metal sealers,
 and it permitted heating up to 300-400°C during the conditioning
 period. Evacuation was accomplished by an oil pump with Fe_2O_3
 adsorption trap, as well as by a titanium electric discharge pump.
 The chamber, together with the discharge cell, were set into the
 gap of an electromagnet with a tip diameter of 25 cm and height
 of 6 cm. The uniform magnetic field in the gap could reach values
 of 2700 A/m. Magnet power supply was from storage batteries.

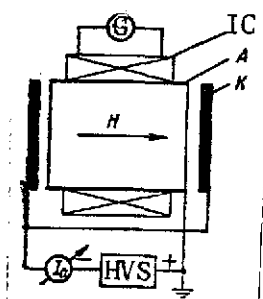


Fig. 1. Diagram of experimental unit: K - cathode; A - anode; IC - measurement coil; G - galvanometer; I_a - microammeter; HVS - high voltage source; horizontal arrow indicates direction of external magnetic field.

An electrical diagram of the unit is presented in Fig. 1. High voltage up to 6 kV is supplied to cathode K of the discharge cell, anode A is at ground potential and it supports measuring magnetic probe IC on the outside. The cell discharge current was measured by instrument I_a (in this case, monitoring for the absence of a separate current on the chamber walls was carried out), and the diamagnetism of the plasma generated

in the discharge cell was measured by magnetic probe IC, by means of galvanometer G. In order to eliminate the effect of random fluctuations of the magnetic field, a compensator, connected towards and located outside the anode, was connected in series with the measurement coil, located on the anode. Upon turning off the high voltage, the plasma broke down, and the anode coil recorded only the change in magnetic field due to disappearance of the

plasma diamagnetism. The magnetic probe was calibrated with a special single-wound coil, through which a fixed current passed and the dependence of the galvanometer deflection on the magnetic field strength or on the current was formed.

Measurement Results

In the case of a Penning discharge, the conditions for formation of a diamagnetic moment in the plasma filling the cylindrical anode cavity are quite well satisfied. The absence of thermodynamic equilibrium between the plasma and the container walls is necessary for existence of diamagnetism [4]. This takes place in a high voltage Penning discharge, since the electrons falling on the anode are not reflected from it and do not create a secondary electron emission and since the magnetic field is parallel to the anode surface and the inhibiting electric field is perpendicular to it. Thus, the anode is an ideal black body for the incident electrons. In this case, the elementary orbital currents on the anode surface remain uncompensated and can be represented by a certain "envelope" surface current. This current creates the diamagnetic moment /29

$$M = -I \cdot S = -\frac{SnkT}{H}, \quad (1)$$

where S is the cross section area of the cylindrical plasma column, with a height equal to the unit length; n and T are the density and temperature of the plasma; k is the Boltzmann constant and H is the magnetic field.

On the other hand, the following magnetostatic equilibrium equation can be written down for the plasma:

$$\frac{H_1^2}{8\pi} = \frac{H_0^2}{8\pi} - nkT, \quad (2)$$

where H_0 is the external magnetic field and H_1 is the field inside the plasma. It must be noted that, since the plasma is considered to be a combination of particles and the magnetic field is distorted little because of diamagnetism, by transforming (2), we can write

$$nkT = \frac{\Delta H \cdot H_0}{4\pi} = q. \quad (3)$$

In this work, principally the values of ΔH were measured, by means of which the following plasma parameters were estimated: energy content, density, temperature, as well as the dependence of these parameters on external factors.

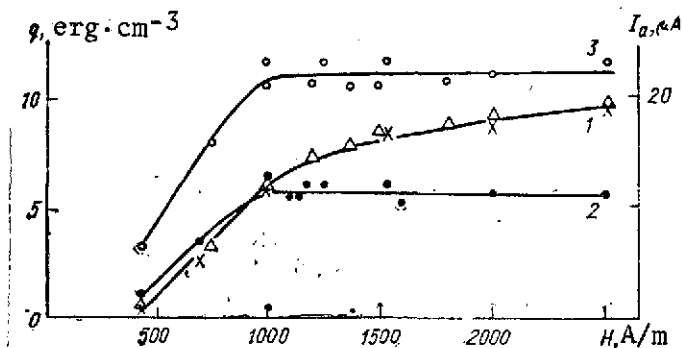


Fig. 2. Diamagnetism (curve 1) and discharge current (curves 2 and 3) vs. magnetic field; experimental points \times , \bullet correspond to a pressure of $3.8 \cdot 10^{-7}$ torr and Δ to a pressure of $8.3 \cdot 10^{-7}$ torr; the working gas is air; applied voltage $U_a = 5.6$ kV.

Thus, plasma energy content vs. magnetic field is presented in Fig. 2. Points are plotted on the graph for two pressures, the one double the other; however, they lie practically on a single curve. This /30 indicates that the pressure of the neutral gas is not determinative, at least in the pressure region indicated. Moreover, it is evident that the value of the diamagnetism, beginning at a certain magnetic field value, tends

towards saturation. The discharge currents reach saturation and, for pressures at which one is double the other, their ratio is two.

The effect of other factors was studied further, in the region in which q does not depend on the magnetic field or depends weakly on it.

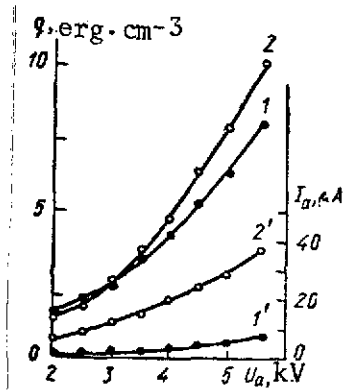


Fig. 3. Diamagnetism (curves 1 and 2) and discharge current (curves 1' and 2') vs. applied voltage; curves 1 and 1' for $p = 1.8 \cdot 10^{-7}$ torr, curves 2 and 2' for $p = 1.8 \cdot 10^{-6}$ torr; magnetic field $H = 2000$ A/m.

It is evident from Fig. 3 that diamagnetism depends strongly on the applied voltage. In this case, the dependence on voltage is clearly nonlinear, which indicates an increase in not only energy of the particles responsible for the diamagnetism, but an increase in density of these particles, since there is no basis for assuming that the ratio of transformation of the applied voltage to the transverse energy of the particles can change

with increase in voltage. A comparison of curves 1 and 2 shows that, for neutral gas pressures differing by a factor of 10, the discharge currents differ by 5 times, while the difference for curves characterizing the diamagnetism behavior is approximately 10-15%. Thus, Figs. 2 and 3 show that the principal factor determining the diamagnetism value is the discharge voltage.

In study of diamagnetism, the absolute value of the plasma energy content or noncompensated current circulating close to the anode surface I_c is measured. It follows from expressions (1) and (3) that

$$I_c = \frac{nkT}{H_0} = \frac{\Delta H}{4\pi} \quad (4)$$

and it will depend on U_a , just like q .

It is clear from the curves of Fig. 4 that the circulating current increases extremely rapidly with applied voltage, and that this dependence is nonlinear and proportional to U_a^b , where $b > 1$. It can be concluded from this that the surface density of the current increases and, consequently, the plasma density overall increases.

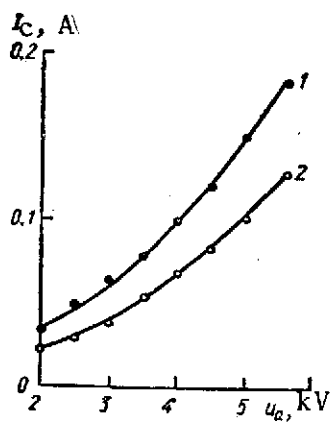


Fig. 4. Circulating current I_c vs. applied voltage U_a ; curve 1 for $H = 1000$ A/m, curve 2 for 2000 A/m; $p = 1.8 \cdot 10^{-7}$ torr, the working gas is air.

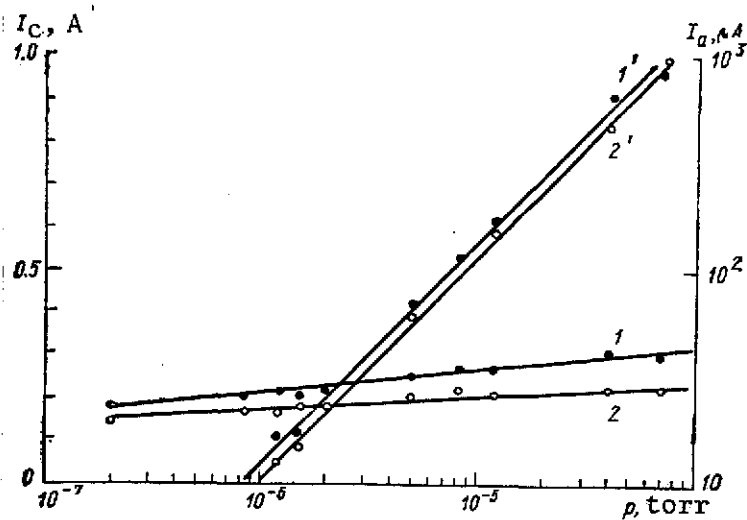


Fig. 5. Circulating current I_c (curves 1 and 2) and discharge current I_a (curves 1' and 2') vs. pressure; working gas is air; curves 1 and 1' for $H = 1100$ A/m and curves 2 and 2' for $H = 2000$ A/m.

A study of the currents flowing in the discharge is shown in Fig. 5. The behavior of the discharge current corresponds well to the manometric properties of the discharge, in a pressure change by a factor of 2; in this case, the circulating current changes by less than a factor of 2. The ratio of the circulating current to the discharge for a large pressure

range is presented in Fig. 6. It is seen that, at very low pressures, this ratio can reach values on the order of 10^5 . The latter fact is very important, since it indicates a long lifetime of the particles in the section.

Circulating current vs. magnetic field strength is presented in Fig. 7.

The curves obtained for a wide pressure range duplicate the basic traits of each other. Only two of them are presented. Linear growth, then a certain unstable maximum (reproducibility of the measured value deteriorates) and a smooth drop are common to all of them.

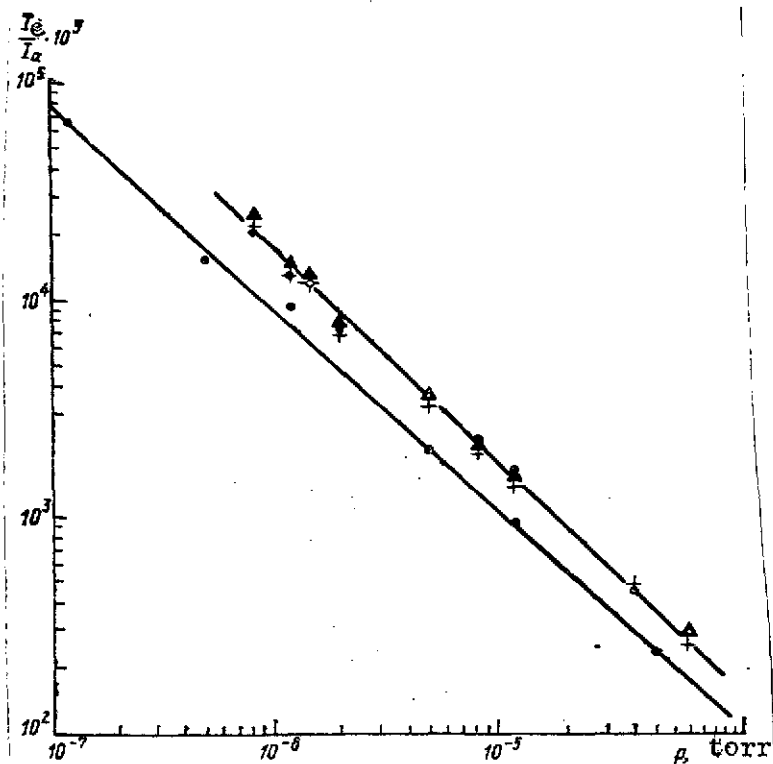


Fig. 6. Ratio of circulating current to discharge vs. pressure; upper curve for hydrogen at $H = 1100, 1500$ and 2000 A/m; lower curve for air; applied voltage $U_a = 5.5$ kV.

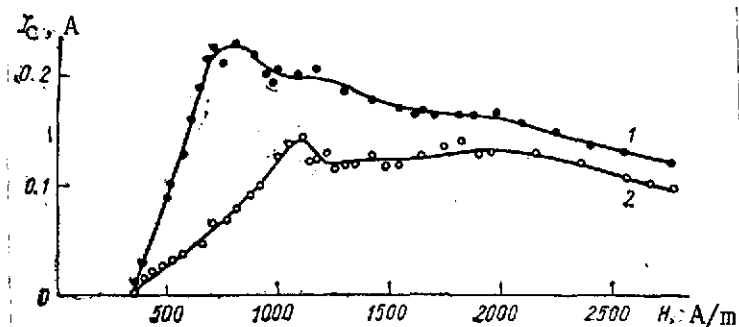


Fig. 7. Circulating current I_c vs. magnetic field; curve 1 for $p = 1.2 \cdot 10^{-6}$ torr, curve 2 for $p = 1.2 \cdot 10^{-7}$ torr; $U_a = 6$ kV, working gas is air.

The discharge ^{/32} behaves quite stably in our experiments, beginning with a field of 1500 A/m. A slight decrease in circulating current is observed in this region. The reasons for this behavior apparently is change in the trajectories of the charge particles with increase in magnetic field.

Study of the cathode sputtering patterns in the discharge cell are of great importance in interpretation of the results. In this case, the symmetry of these patterns and their reproducibility from test to test should be noted; this is evidence of reflection by them of highly characteristic traits of the movement of

ions (Fig. 8). The following method was used to visualize these patterns. A copper layer, approximately 10^3 Å thick, was sputtered

onto the aluminum cathode. For discharge conditions $U_a = 3000$ V, $H_0 = 2500$ A/m, $p \sim 1 \cdot 10^{-6}$ torr, after several hours of operation of the cell, a quite true circular shape about 1 mm in diameter in the central region of the cathode proved to be unsputtered, while the copper layer in the vicinity was completely removed and the aluminum surface was bare. The outer diameter of the visible aluminum ring was about 2 mm. A region of weaker sputtering of the copper coating followed, up to a diameter of 3 mm. The proposal was expressed in work [3] that these sputtering shapes are connected with formation and acceleration of ions in regions directly in contact with the anode, in which the accelerating field is quite rigidly radial. The ions accelerated by this field move in a cycloid in it, and they cannot intersect a certain near-axial region, the radius of which depends on the magnetic field strength, ion mass, accelerating field strength and anode diameter. /33

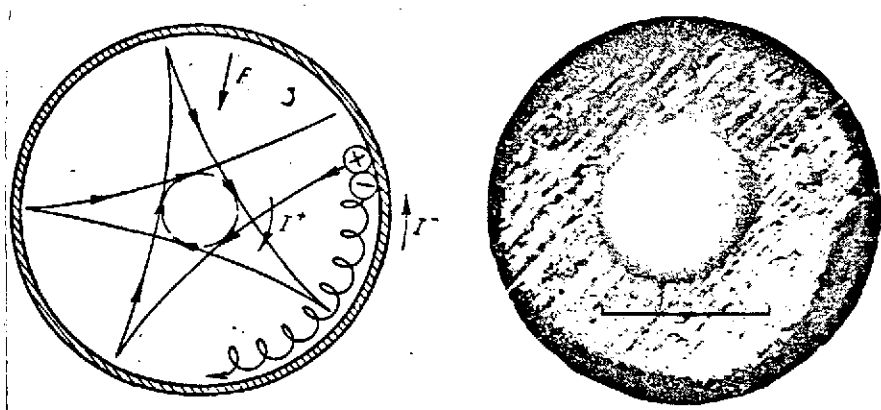


Fig. 8. Diagram of movement of charged particles in a discharge, in a plane perpendicular to the magnetic field, on the left, and sputtering pattern in the central part of the cathode, on the right; unsputtered sections in the center and on the periphery.

Let us estimate the size of the unsputtered spot. We assume that the total potential drop takes place in the layer next to the anode. Disregarding the size of this layer, in comparison with

the anode cylinder radius, we will consider that ions formed in this layer have an initial velocity $v_0 = \sqrt{\frac{2eU_a}{m_i}}$, directed along the radius, and it moves under the action of the magnetic field alone:

$$m_i \frac{dv}{dt} = \frac{e}{c} [\mathbf{vH}].$$

Using cylindrical coordinates, we integrate this equation with the initial conditions: $t = 0$, $r = r_a$, $v_r = v_0$ and $d\phi/dt = 0$. We obtain

$$r^2 = \frac{2v_0}{\omega_H} \sqrt{r_a^2 + \frac{v_0^2}{\omega_H^2}} \sin\left(\frac{\omega_H t}{4} + \alpha\right) + \frac{2v_0^2}{\omega_H^2} + r_a^2,$$

where $\omega_H = \frac{eH}{m_i c}$ и $\alpha = -\arcsin \frac{v_0}{\omega_H \sqrt{r_a^2 + \frac{v_0^2}{\omega_H^2}}}$.

The radius r will have the minimum value when $\sin\left(\frac{\omega_H t}{4} + \alpha\right) = -1$, /34
then

$$r_{\min}^2 = \left(\sqrt{r_a^2 + \frac{v_0^2}{\omega_H^2}} - \frac{v_0}{\omega_H} \right)^2.$$

Introducing $r_c = v_0/\omega_H$, we obtain

$$r_{\min} = \sqrt{r_a^2 - r_c^2} - r_c, \quad (5)$$

where r_a is the anode radius, and r_c is the Larmor radius of the ion. The same result can be obtained by a geometric plot of the trajectory of the movement of an ion within the anode.

A diagram demonstrating the movement of ions in a plane perpendicular to the anode cross section is presented in Fig. 8. In the process of ionization, ions can acquire a certain random energy, on the order of several electron volts, including along

the direction of the magnetic field, which permits them to drift with a certain longitudinal velocity in the direction of the cathode. Upon impact with the cathode, however, the total energy of the ions is realized.

Thus, under the experimental conditions $U_a = 3000$ V, $H_0 = 2500$ A/m, $r_a = 1$ cm and working gas, air, the ion energy was calculated from the sputtering patterns: $E_{\max} = 2800 \pm 300$ eV; $E_{\min} = 580 \pm 45$ eV. The calculation was carried out from the diameter of the region of the complete atomization ring of the copper. The inner diameter (~ 0.95 mm) corresponds to the maximum energy and the outer (~ 2.1 mm) to the minimum. In order to obtain the energy distribution of the ions, the measurements made were not sufficient, since an energy correction must be introduced into the sputtering value.

From the fact that ions acquire an energy comparable to the /35 potential applied to the discharge, it can be concluded that, first, there is an electric field in which an ion can acquire such energy, second, the electric field is perpendicular to the anode and third, since the electrical field is created by the space charge electrons, the energy of the electrons in the cloud is comparable to the applied voltage value.

Thus, knowing the absolute value of the energy included in the plasma and the estimated electron energy, the lower limit of the plasma density can be obtained. A curve of the lower density limit vs. discharge voltage is presented in Fig. 9, from which it is seen that the density is low and only exceeds 10^9 cm⁻³ at the maximum discharge voltage. If it is assumed that the charge of the electrons is uncompensated, knowing the volume of the discharge cell (~ 8 cm³), the total number of electrons can be calculated. It proves to be $\sim 10^{10}$ particles. This amount is insufficient to create a space charge potential close to the applied voltage.

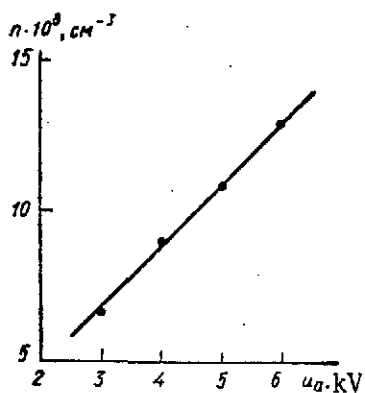


Fig. 9. Plasma density vs. applied voltage: $p = 3.6 \cdot 10^{-6}$ torr, $H = 2000$ A/m, working gas is hydrogen.

The density necessary for this must be approximately 4-5 times greater. Concerning this non-correspondance, the suggestion can be expressed that there is a systematic error in measurement of the diamagnetism.

Hypothesis 1: the uncompensated current is further from the inner surface of the cathode than the Larmor radius of the electrons

(the calibration was made for a distance approximately equal to the Larmor radius with intermediate values of the applied voltage); hypothesis 2: it is seen from Fig. 8 that an ion current flows around the axis inside the cell, the direction of which is opposite to that of the diamagnetic current flowing next to the anode.

The radial portion of the ion trajectories, as is seen from the 36 diagram, makes no contribution, since it is mutually compensated. Next to the anode, the ions decrease speed to zero, owing to the inhibiting electric field. Therefore, this part of the trajectory also makes no contribution to the magnetic moment of the discharge plasma. Thus, only the near-axial ion current creates the paramagnetic effect and, since the measurement is made by means of a coil encompassing the entire cell, in measurement of the diamagnetism and the circulating current, the values may be understated. The observed decreasing dependence of the circulating current on magnetic field (see Fig. 7) apparently can be explained by a decrease in the Larmor radii of the ions r_c and with departure of the enveloping ion current from the axis. In principle, with very strong magnetic fields, the ion current can approach so close to the circulating electron that it completely liquidates the plasma diamagnetism. In this manner, the measured values of the diamagnetism give us only a lower limit of the plasma energy content and the value of I_c . Therefore, in order to obtain more

precise values, direct measurements of the plasma density and particle energy distribution are necessary.

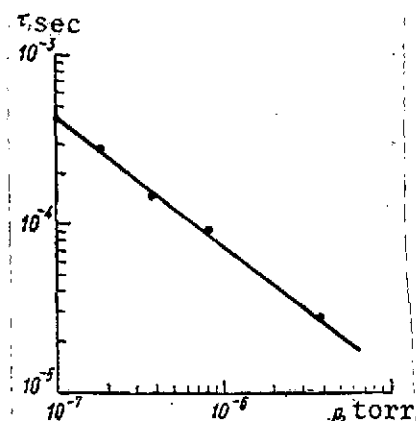


Fig. 10. Energetic plasma lifetime vs. pressure: $U_a = 3$ kV, $H = 2500$ A/m, working gas is air.

Even with such understated measurements of the diamagnetism, there is interest in examining the behavior of the energetic plasma lifetime in the system being studied. The energetic lifetime τ is understood to be the time for departure of the energy accumulated in the system, at a certain minimum steady power supplied to the system:

$$\tau = \frac{q \cdot V}{I_a \cdot U_a}, \quad (6)$$

where V is the cell volume, q is the energy content per cm^3 . The dependence of τ on pressure is presented in Fig. 10, from which it is seen that the plasma lifetime can reach 300 μsec , at a pressure on the order of 10^{-7} torr. This is under conditions, when the system apparently has no confining properties, from the point of view of traditional devices.

The plasma breakdown can take place, in particular, owing to certain elementary processes, ionizing collisions and recharging. If the free path time of an electron until an ionizing collision τ_{ion} and the ion recharging time τ_{re} are compared, it appears that τ_{ion} is at least 100 times less than the recharging time.

For electron energies of about 3000 eV in nitrogen, $\sigma_{\text{ion}} = 3.86 \cdot 10^{-17} \text{ cm}^2$ [5]. At $p = 2 \cdot 10^{-7}$ torr, $\tau_{\text{ion}} = 5.5 \cdot 10^{-4} \text{ sec}$,

which is two times greater in all than the observed time (Fig. 10). This can be considered to be a good coincidence, within the limits of accuracy of measurements of the neutral gas pressure in the region of the discharge cell.

Thus, ionization collisions apparently are the basic process in loss of particles and energy from the system.

REFERENCES

/37

1. Bobykin, B.V., V.M. Kel'man, and L.M. Nazarenko, ZhTF 38/3, 194 (1968).
2. Schuurman, W., Physica 36, 136 (1967).
3. Knauer, W., J. Appl. Phys. 33, 2093 (1962).
4. Alfven, H. and K.G. Fel'tkhammar, Kosmicheskaya elektrodinamika [Space electrodynamics], Mir Press, Moscow, 1967, p. 237.
5. Schram, B.L., F.J. DeHeer, M.J. Van der Wiel, and Y. Kistemaker, Physica 31/1, 94 (1965).